

# Metal clad active fibres for power scaling and thermal management at kW power levels

JAE M. O. DANIEL,<sup>1,2,\*</sup> NIKITA SIMAKOV,<sup>1,3</sup> ALEXANDER HEMMING,<sup>1</sup>  
W. ANDREW CLARKSON,<sup>3</sup> AND JOHN HAUB<sup>1</sup>

<sup>1</sup>Laser Technologies Group, Cyber and Electronic Warfare Division, Defence Science and Technology Group, Department of Defence, Edinburgh, South Australia 5111, Australia

<sup>2</sup>Aether Photonics, Adelaide, Australia

<sup>3</sup>Optoelectronics Research Centre, University of Southampton, Highfield, SO17 1BJ, UK

\*Jae.Daniel@dsto.defence.gov.au

**Abstract:** We present a new approach to high power fibre laser design, consisting of a polymer-free all-glass optical fibre waveguide directly overlaid with a high thermal conductivity metal coating. This metal clad active fibre allows a significant reduction in thermal resistance between the active fibre and the laser heat-sink as well as a significant increase in the operating temperature range. In this paper we show the results of a detailed thermal analysis of both polymer and metal coated active fibres under thermal loads typical of kW fibre laser systems. Through several different experiments we present the first demonstration of a cladding pumped aluminium-coated fibre laser and the first demonstration of efficient operation of a cladding-pumped fibre laser at temperatures of greater than 400 °C. Finally, we highlight the versatility of this approach through operation of a passively (radiatively) cooled ytterbium fibre laser head at an output power of 405 W in a compact and ultralight package weighing less than 100 g.

©2016 Optical Society of America

**OCIS codes:** (140.3510) Lasers, fiber; (140.6810) Thermal effects.

## References and links

1. D. J. Richardson, J. Nilsson, and W. A. Clarkson, "High power fiber lasers: current status and future perspectives," *J. Opt. Soc. Am. B* **27**(11), B63 (2010).
2. K. Tankala, D. Guertin, J. Abramczyk, and N. Jacobson, "Reliability of low-index polymer coated double-clad fibers used in fiber lasers and amplifiers," *Opt. Eng.* **50**(11), 111607 (2011).
3. F. Beier, C. Hupel, J. Nold, S. Kuhn, S. Hein, J. Ihring, B. Sattler, N. Haarlammer, T. Schreiber, R. Eberhardt, and A. Tünnermann, "Narrow linewidth, single mode 3 kW average power from a directly diode pumped ytterbium-doped low NA fiber amplifier," *Opt. Express* **24**(6), 6011–6020 (2016).
4. A. Méndez and T. Morse, *Specialty Optical Fibers Handbook* (2011).
5. J. M. O. Daniel, N. Simakov, A. Hemming, W. A. Clarkson, and J. Haub, "Ultra-high temperature operation of a tunable ytterbium fibre laser," in *Eur. Conf. Lasers Electro-Optics* (2015), paper CJ\_11\_6.
6. J. M. O. Daniel, N. Simakov, A. Hemming, W. A. Clarkson, and J. Haub, "Passively cooled 405 W ytterbium fibre laser utilising a novel metal coated active fibre," *Proc. SPIE* **9728**, 972808 (2016).
7. C. X. Yu, O. Shatrovov, and T. Y. Fan, "All-glass fiber amplifier pumped by ultrahigh brightness pump," *Proc. SPIE* **9728**, 972806 (2016).
8. Y. Jeong, J. Nilsson, J. K. Sahu, D. N. Payne, R. Horley, L. M. B. Hickey, and P. W. Turner, "Power scaling of single-frequency ytterbium-doped fiber master-oscillator power-amplifier sources up to 500 W," *IEEE J. Sel. Top. Quantum Electron.* **13**(3), 546–550 (2007).
9. J. W. Dawson, M. J. Messerly, R. J. Beach, M. Y. Shverdin, E. A. Stappaerts, A. K. Sridharan, P. H. Pax, J. E. Heebner, C. W. Siders, and C. P. J. Barty, "Analysis of the scalability of diffraction-limited fiber lasers and amplifiers to high average power," *Opt. Express* **16**(17), 13240–13266 (2008).
10. B. J. Skutnik, B. Foley, and K. B. Moran, "High-numerical-aperture silica core fibers," *Proc. SPIE* **5317**, 39–45 (2004).
11. "For example 150 W into 105 0.15 NA @915 nm from BWT Beijing LTD," <http://www.bwt-bj.com/>.
12. "For example 1200 W into 300 0.22 NA @975 nm from DiLas GmbH," [www.dilas.com/](http://www.dilas.com/).
13. D. A. Gruk, A. S. Kurkov, V. M. Paramonov, and E. M. Dianov, "Effect of heating on the optical properties of Yb<sup>3+</sup>-doped fibres and fibre lasers," *Quantum Electron.* **34**(6), 579–582 (2004).
14. J. Hansryd, F. Dross, M. Westlund, P. A. Andrekson, and S. N. Knudsen, "Increase of the SBS threshold in a short highly nonlinear fiber by applying a temperature distribution," *J. Lightwave Technol.* **19**(11), 1691–1697 (2001).

15. M. Lapointe, S. Chatigny, M. Piché, M. Cain-Skaff, and J. Maran, "Thermal Effects in High Power CW Fiber Lasers," *Proc. SPIE* **7195**, 71951U (2009).
16. Y. Fan, B. He, J. Zhou, J. Zheng, H. Liu, Y. Wei, J. Dong, and Q. Lou, "Thermal effects in kilowatt all-fiber MOPA," *Opt. Express* **19**(16), 15162–15172 (2011).
17. G. D. Goodno, L. D. Book, and J. E. Rothenberg, "600-W, Single-Mode, Single-Frequency Thulium Fiber Laser Amplifier," *Proc. SPIE* **7195**, 71950Y (2009).
18. H. J. Otto, F. Stutzki, N. Modsching, C. Jauregui, J. Limpert, and A. Tünnermann, "2 kW average power from a pulsed Yb-doped rod-type fiber amplifier," *Opt. Lett.* **39**(22), 6446–6449 (2014).
19. M. Leich, F. Just, A. Langner, M. Such, G. Schötz, T. Eschrich, and S. Grimm, "Highly efficient Yb-doped silica fibers prepared by powder sinter technology," *Opt. Lett.* **36**(9), 1557–1559 (2011).
20. A. Langner, M. Such, G. Schötz, S. Grimm, F. Just, M. Leich, C. Mühlig, J. Kobelke, A. Schwuchow, O. Mehl, O. Strauch, R. Niedrig, B. Wedel, G. Rehmann, and V. Krause, "New developments in high power fiber lasers based on alternative materials," *Proc. SPIE* **7914**, 79141U (2011).
21. S. W. Moore, T. Barnett, T. A. Reichardt, and R. L. Farrow, "Optical properties of Yb<sup>3+</sup>-doped fibers and fiber lasers at high temperature," *Opt. Commun.* **284**(24), 5774–5780 (2011).
22. T. C. Newell, P. Peterson, A. Gavrielides, and M. P. Sharma, "Temperature effects on the emission properties of Yb-doped optical fibers," *Opt. Commun.* **273**(1), 256–259 (2007).
23. J. M. O. Daniel, N. Simakov, A. Hemming, W. A. Clarkson, and J. Haub, "A double clad ytterbium fibre laser operating at 400°C," *Proc. SPIE* **9344**, 934414 (2015).
24. J. M. O. Daniel, "Wavelength selection and transverse mode control in high power fibre lasers," Ph.D Thesis, University of Southampton (2013).
25. M. Meier, V. Romano, and T. Feuer, "Material processing with pulsed radially and azimuthally polarized laser radiation," *Appl. Phys. A* **86**(3), 329–334 (2007).
26. D. Lin, J. M. O. Daniel, M. Gecevičius, M. Beresna, P. G. Kazansky, and W. A. Clarkson, "Cladding-pumped ytterbium-doped fiber laser with radially polarized output," *Opt. Lett.* **39**(18), 5359–5361 (2014).
27. J. Vetrovec, A. S. Litt, D. A. Copeland, J. Junghans, and R. Durkee, "Liquid metal heat sink for high-power laser diodes," *Proc. SPIE* **8605**, 86050E (2013).
28. S. Patterson, T. Koenning, B. Kohler, S. Ahlert, A. Bayer, H. Kissel, H. Muntz, A. Noeske, K. Rotter, A. Segref, M. Stoiber, A. Unger, P. Wolf, and J. Biesenbach, "Enhanced fiber coupled laser power and brightness for defense applications through tailored diode and thermal design," *Proc. SPIE* **8381**, 83810L (2012).
29. J. Campbell, T. Semenic, P. Leisher, A. Bhunia, M. Mashanovitch, and D. Renner, "980nm diode laser pump modules operating at high temperature," *Proc. SPIE* **9730**, 97300G (2016).
30. F. Stutzki, C. Gaida, M. Gebhardt, F. Jansen, A. Wienke, U. Zeitner, F. Fuchs, C. Jauregui, D. Wandt, D. Kracht, J. Limpert, and A. Tünnermann, "152 W average power Tm-doped fiber CPA system," *Opt. Lett.* **39**(16), 4671–4674 (2014).

## 1. Introduction

High power fibre lasers have experienced remarkable uptake within the industrial and defence communities over the last decade [1]. This rapid adoption is due to the beneficial combination of robust single mode operation, power scalability into the multi-kW regime and very high wall plug efficiency. In part this growth has been due to the combination of simplified thermal management and high laser slope efficiencies typically seen in the fibre laser architecture, but is also a result of a sustained and innovative engineering effort from both the academic and commercial laser communities.

A major and continuing challenge to high power fibre laser design has been in the management of losses and heating throughout the length of the active fibre. A point of particular sensitivity is the passive to active fibre fusion splice. Here the combination of several fibre handling steps, the requirement to first strip and then recoat the active and passive fibres, added to the high thermal load of this initial doped section result in an extremely challenging engineering problem. These effects are further compounded by the desire to develop higher output powers and shorter fibre device lengths. Despite many iterations and improvements of the coating process [2], it still remains a limiting feature in the operation of many high power fibre lasers [3].

Typical double clad active fibres consist of a rare earth doped core surrounded by a pure silica inner cladding and low refractive index fluoropolymer outer cladding. Here the fluoropolymer outer cladding is chosen due to its low refractive index and is needed to enable pump light guidance within the inner cladding. However these fluoropolymers show a high degree of thermal sensitivity (low maximum operating temperature) and low thermal conductivity. This results not only in an insulating barrier for heat removal but also represents

a point of maximum sensitivity to fibre operating temperature, being prone to thermal damage and failure. This high sensitivity, low damage threshold fluoropolymer presents significant challenges to fibre reliability. In this context the fluoropolymer coating can be seen as a weak point within the laser or amplifier, degrading at temperatures above  $\sim 80^{\circ}\text{C}$ . With appropriate fibre designs it is possible to remove the requirement for using this fluoropolymer coating and open up the way for new and novel fibre laser architectures. For example replacing the outer cladding with materials that exhibit more desirable properties such as high thermal conductivity and higher temperature handling, can have a number of benefits. Metal coated optical fibres, where the outer protective coating comprises a thin metal layer rather than a polymer, have been used in harsh-environment sensing applications for more than two decades [4]. However, only recently have they been demonstrated in cladding pumped active fibre configurations.

First presented at the CLEO Europe conference [5], metal coated all-glass active fibres possess a number of benefits, such as several orders of magnitude increased thermal conductivity, significantly increased upper temperature limits as well as demonstrated static fatigue and pull strength values almost twice that of polymer coated fibre [4]. More recently, their significant potential for power scaling has been highlighted by both ourselves [6] and Yu et al. [7]. In this work we present the first detailed analysis of the thermal and optical properties of metal coated active fibres for power scaling and harsh environment use.

The use of metal coatings on cladding pumped active fibres was first proposed by Jeong et al. as a route to improved stimulated Brillouin scattering (SBS) suppression in microstructured fibres through an increased thermal gradient [8]. This was proposed in the context of air jacketed microstructured fibres where the requirement of light guiding polymer coatings does not exist, however such designs have presented challenges in the multi-kW single mode regime. Dawson et al. [9] later briefly proposed a similar approach (this time using a low refractive index all-glass outer cladding) as a way to bypass the temperature handling limitations of fluoropolymer claddings. However, other than these initial proposals this approach was not pursued. This lack of progress can be understood in the context of the increased diode brightness requirements for all-glass claddings. Typically all-glass triple-clad fibres have cladding NA's in the range of 0.22 – 0.28 (although index contrasts of up to  $\sim 0.4 - 0.5$  have been demonstrated in all-glass passive fibres [10]), this is in comparison to the  $\sim 0.46$  NA regularly seen in fluoropolymer coatings. Because of this, diode brightness requirements are typically much larger for the all-glass claddings. Previously this higher brightness requirement meant that such an approach was not a feasible option for kW systems; however diode brightness has since increased dramatically with available diode brightness no longer limiting the power scalability of high power fibre sources. Indeed, the current state of the art diode brightness levels exceed  $10 - 25 \text{ MW sr}^{-1} \text{ cm}^{-2}$  [11,12] and correspond to theoretical pump powers of 10 to 25 kW coupled into a  $400 / 0.46$  optical fibre. The dramatic increase in diode brightness as well as a continuing trend of lower cost per watt, even for the highest brightness pump modules opens up the possibility of kW level fibre lasers operating with relatively low NA cladding guides.

Another interesting benefit of moving to high temperature handling fibre coatings is the ability to withstand a much greater range of operating temperatures. This can be of benefit for increased wavelength tunability [13], improved laser cooling performance and increased thresholds for detrimental nonlinear processes such as SBS where an estimated increase in threshold of  $\sim 2\text{dB}$  per  $100^{\circ}\text{C}$  of temperature variance is achievable [14]. In this paper we for the first time analyse several major advantages that come with the use of metal coated active fibres such as increased fibre operating ranges, reduction in peak core temperature and potential for significantly increased thermal loads. This analysis is experimentally validated, initially at low powers and then with the first demonstration of a passively (radiatively) cooled fibre laser operating at up to 405 W of output power.

## 2. Background

A typical optical fibre laser / amplifier configuration is shown schematically in Fig. 1. An array of fibre coupled pump diodes is coupled into a double clad fibre via the use of a pump beam combiner with signal feed-through. This combined output is then spliced to a length of rare earth doped active fibre; here the coupled pump power is absorbed by the laser active medium over a number of meters and eventually converted to laser light. Although on average such a configuration results in mean thermal loads greatly reduced in comparison to bulk laser systems there are several points of very high thermal load such as the diode to optical fibre coupling, the passive to active fibre fusion splice and the distributed length of active fibre used as the laser gain medium. In this section we will analyse the required thermal performance of the active fibre and active fibre mounting arrangements, looking at the benefits of moving towards more robust and higher performance optical fibre coatings.

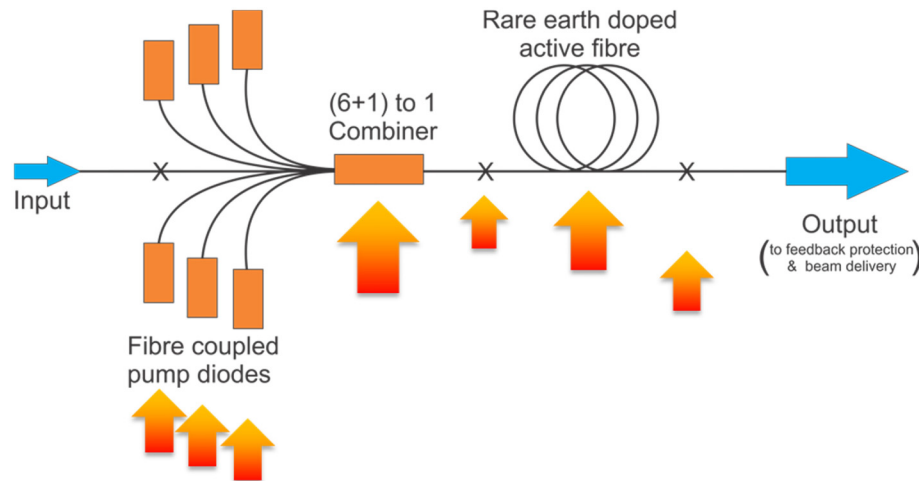


**Fig. 1.** A simplified fibre laser / amplifier arrangement with arrows indicating the typical points of high thermal load within the laser chain.

### 2.1. Active fibre and heatsink design

Here the thermal performance of both metal and polymer coated active fibre is investigated. Adopting an industry standard dimension for polymer cladding thickness of 75  $\mu\text{m}$  and a metal coating thickness of 30  $\mu\text{m}$  we compare fibres based on inner cladding diameter over a range of 100  $\mu\text{m}$  to 500  $\mu\text{m}$ . For all-fibre designs a fixed core diameter of 20  $\mu\text{m}$  is assumed and an octagonally shaped inner cladding is chosen to enable pump light scrambling and reduced device lengths. For the industry standard fibre diameters of 250 and 400  $\mu\text{m}$  this results in a polymer coated fibre of core / inner cladding and outer polymer coating of 20/250/400  $\mu\text{m}$  and 20/400/550  $\mu\text{m}$  respectively. For the metal coated active fibre a fixed ratio of inner cladding to fluorine doped glass outer cladding is assumed at 1:1.15 and results in core, inner cladding, fluorine doped glass outer cladding and metal coatings of 20/250/290/350  $\mu\text{m}$  & 20/400/460/520  $\mu\text{m}$  respectively. End face profiles of these two fibre designs are shown in Fig. 2(a) and Fig. 2(b).

For high power laser systems, active fibre is typically placed in thermal contact with a cooled heatsink [15,16]. Figure 2(c) shows a simplified implementation of this, consisting of a water cooled aluminium plate with rectangular shaped trenches machined into the surface. Due to manufacturing tolerances in both the slot width and the active fibre coating thickness, it is preferential to machine this slot slightly oversize and use a thermally conductive filler material to enable heat conduction. For the active fibres described above we assume a slot width 0.2 mm greater than the fibre outer diameter. i.e. slot dimensions of 750  $\mu\text{m}$  x 750  $\mu\text{m}$

for an outer fibre diameter of 550  $\mu\text{m}$ . In all cases the heatsink design featured an aluminium capping layer for added heat removal. Both capping layer and body were assumed to be at a fixed heatsink temperature 20°C (typically achieved using water channel cooling). For both fibre types we assume ideal thermal contact between the optical fibre glass, cladding and interstitial material. To account for localised roughness of the slot and active fibre, the fibre is assumed to be mounted with a 5  $\mu\text{m}$  offset from the base of the slot. This is equivalent to assuming an interface thermal resistance equal to the fibre offset divided by the interstitial material thermal conductivity.

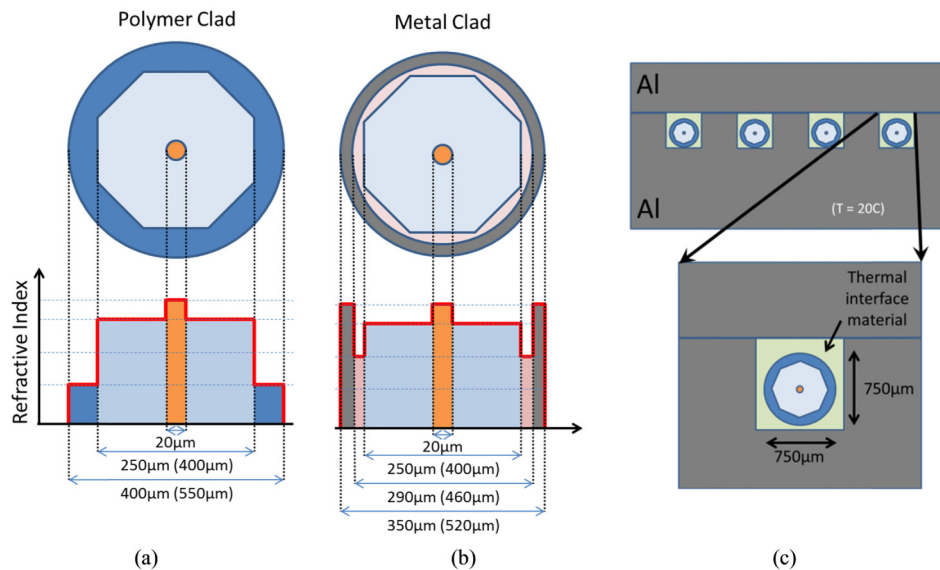


**Fig. 2.** a) polymer clad active fibre with core, inner cladding and polymer dimensions of 20/250/400  $\mu\text{m}$  (20/400/550  $\mu\text{m}$ ). b) Metal clad active fibre with core, inner cladding, outer cladding and metal dimensions of 20/250/260/350  $\mu\text{m}$  (20/400/460/520  $\mu\text{m}$ ). c) Schematic of 550  $\mu\text{m}$  (OD) active fibre embedded within a water-cooled aluminium heatsink, with slot width of 750 x 750  $\mu\text{m}$  and surrounded by a thermally conductive interface material.

## 2.2. Active fibre thermal modelling and analysis

For these simple fibre and heatsinking geometries, estimates of fibre core temperature and temperature drop across the active fibre were modelled using commercially available finite element modelling software (COMSOL). In Fig. 3 we plot the results of this modelling over the typical design space for high power fibre lasers and is shown as a function of interstitial material thermal conductivity under a fixed thermal load of 100 W/m. Here we can see how polymer coated active fibre shows not only a consistently increased temperature but also a much stronger dependence on interstitial material thermal conductivity.



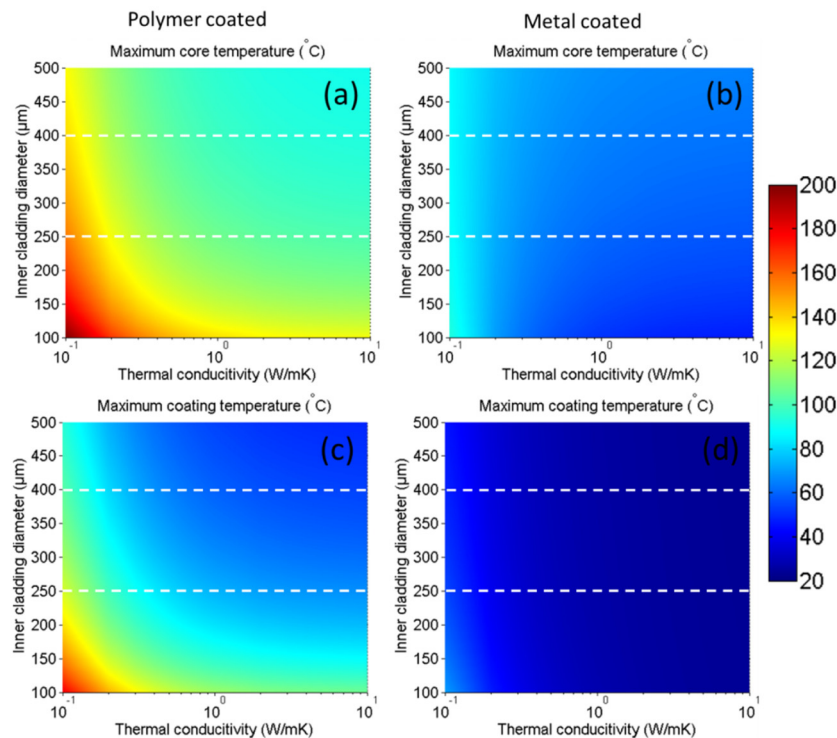


**Fig. 3.** Thermal profiles for polymer coated (left) and metal coated (right) active fibres under a 100W/m thermal load and plotted for a range of interstitial material thermal conductivities. Peak core temperature (top) and peak outer cladding temperature (bottom) are plotted in pseudocolor over a 20 – 200 degree range with scale bar shown on right. Dotted lines indicate the data points used in Fig. 4. The raw data for these plots is available online.

For a polymer coated fibre with a 250  $\mu\text{m}$  cladding diameter a  $\sim 20^\circ\text{C}$  reduction in core temperature is seen by simply moving from a interstitial material thermal conductivity of 0.18 W/mK (typical conductivity of UV curable fluoropolymers) to 1 W/mK. The maximum temperature of the fluoropolymer coating is perhaps a more important metric as this can lead to premature fibre degradation. When ranging from a thermal conductivity of 0.18 W/mK to 1 W/mK the maximum polymer temperature is reduced from  $90^\circ\text{C}$  ( $75^\circ\text{C}$ ) to  $70^\circ\text{C}$  ( $55^\circ\text{C}$ ) for the 250  $\mu\text{m}$  (400  $\mu\text{m}$ ) fibre cladding diameter. Beyond this, increasing the conductivity of the interstitial material has only minimal effect, with the polymer cladding itself acting as an insulator and contributing to the bulk of the temperature increase. For the case of the metal coated active fibre, core and cladding temperature dependence on the thermal conductivity of the interstitial material is greatly reduced. In this case the bulk of thermal resistance is caused by the active fibre glass cladding.

These two behaviours are highlighted in the plots of Fig. 3 with polymer clad active fibre performing better at larger cladding diameter. For the metal coated fibre this situation is reversed, with thinner small diameter fibres outperforming their larger diameter equivalents. Figure 4 details a cross-sectional thermal profile of both the polymer and metal coated active fibres, here we can better compare the reductions in peak core temperatures between the polymer and metal coated fibres. At inner cladding diameters of 250  $\mu\text{m}$  (Fig. 4(a)) and 400  $\mu\text{m}$  (Fig. 4(b)) a drop in peak temperature of 50 and 40  $^\circ\text{C}$  is seen for the metal coated fibres.

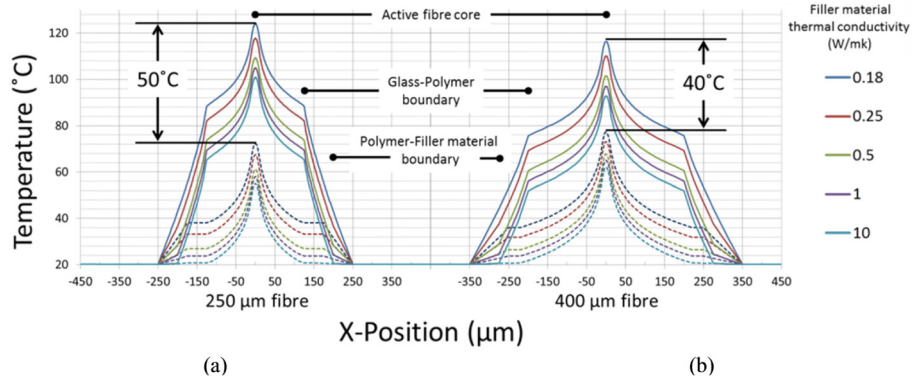


**Fig. 4.** Thermal profiles for polymer coated (solid lines) and metal coated (dashed lines) active fibres under a 100W/m thermal load and plotted for a range of interstitial material thermal conductivities. At an interstitial material thermal conductivity of 0.18 W/mK a 50°C & 40°C reduction in core temperature is seen for the case of a) 250 µm & b) 400 µm metal coated fibres.

For a polymer coated active fibre embedded in thermally conductive interstitial material heat flow tends to be symmetric about the fibre core. This is due to the relatively high thermal resistance on the polymer cladding. For the case of metal coated fibre heat flow is much more concentrated about the regions in close contact with the heat sink. Here the metal coating acts as a heat conduit and is able to transmit a much high degree of heat flux in comparison to the polymer cladding. Figure 5 highlights the difference in thermal flow between the polymer and metal coated fibre designs. Here the end-face view of the active fibre is shown within the cooled heatsink arrangement. These profiles are overlaid with a pseudocolor temperature profile (scale on right) as well as heat flux lines (shown in white). The intensity of the colour profile details temperature and the density of the flux lines details heat flow.

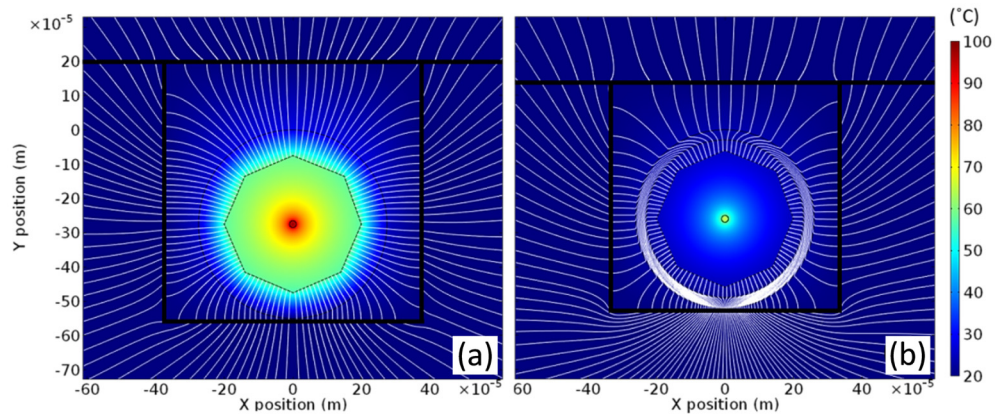


**Fig. 5.** Thermal profiles of a) polymer and b) metal coated fibre lasers under a 100W/m thermal load with an interstitial material thermal conductivity of 1W/mK and 5µm offset from heatsink base. Colour profile details temperature (°C, scale on right) and the density of the flux lines (shown in white) detail heat flow.

For a low gain amplifier and minimal background loss the average thermal load per unit length can be estimated by  $T_h \approx P_0 \eta / L$  where  $P_0$  is the launched pump power,  $\eta$  is the power conversion efficiency and  $L$  is the length of active fibre required for complete pump absorption. Although in practice the thermal load incident on an active fibre is highly dependent on dopant, host composition, losses arising from background absorptions and

splice losses, it is still instructional to look at the effects of W/m heat load as a first order effect.

Figure 6 shows the calculated maximum core (a) and cladding (b) temperatures as a function of active fibre thermal load for a 400  $\mu\text{m}$  diameter active fibre with either polymer cladding (red line) or metal cladding (blue line). Here we can see the significant advantage of moving to metal clad active fibres. As thermal load is increased the difference in temperatures of the two architectures is highlighted. At a thermal load of 300 W/m (as shown in a number of works [17,18]) we can already see an approximately 100 degree reduction in core temperature. Perhaps more importantly, for the polymer clad fibre this thermal load results in a maximum polymer cladding temperature approaching that of thermal failure ( $\sim 100^\circ\text{C}$ ). Significant increases in thermal load beyond this point are impractical for the current generation of polymer coated fibres but well within the capabilities of the metal coated fibre design. Thermal loads of 1 kW/m are feasible using metal coated fibre with the main limitation being the thermal conductivity of the active fibre glass rather than cladding.

Soft glass active fibre and lasers show an even greater sensitivity to thermal load in comparison to their more robust silica counterparts. Here the combination of relatively low melting points, approximately half the thermal conductivity of fused silica and a tendency towards relatively large quantum defect transitions all serve to limit power scaling of these fibres. By moving to a metal clad active fibre thermal loads (and thus output powers) can be pushed beyond what is currently possible and could be a promising route to power scaling within the mid-IR.

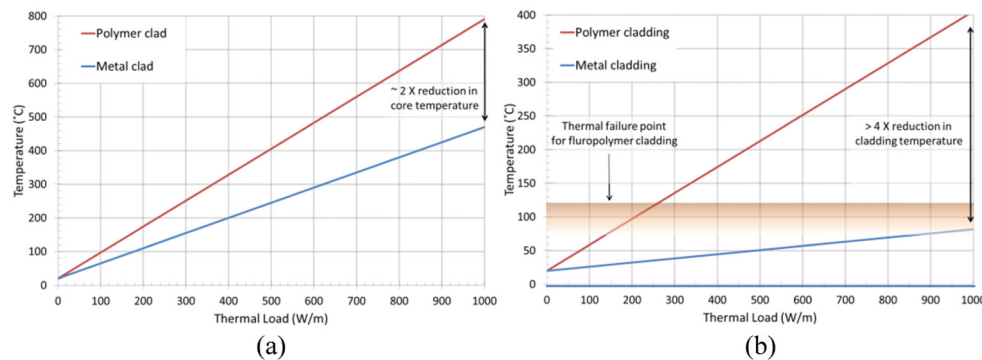


**Fig. 6.** Maximum predicted a) core and b) cladding temperature as a function of thermal load for polymer clad (red) and metal clad (blue) active fibre designs.

Although not discussed in this section an additional advantage of the metal coated active fibre is its ability to be permanently fixed in place using low melting point solder or other phase change material. The excellent thermal contact and high thermal conductivity of these mounting options removes the need for accurately machined fibre grooves or complex heatsink designs whilst effectively reducing the interface resistance to near zero.

### 3. Experimental arrangement

To validate this approach to laser design as well as to gain an insight into the behaviour of rare earth doped fibre lasers at high temperatures, a custom all-glass fibre preform was commissioned and drawn with a metal outer coating.

#### 3.1. Metal coated ytterbium doped active fibre

The active fibre preform used in these experiments was fabricated by Heraeus Quarzglas. This fibre design consisted of a powder sintered fused silica core material [19,20] co-doped with approximately 0.04 wt%  $\text{Yb}_2\text{O}_3$  and 0.8 wt%  $\text{Al}_2\text{O}_3$ . The inner cladding of this fibre was pure fused silica (F300) and shaped octagonal for increased pump absorption and finally overlaid



with a down doped fluorosilicate layer to enable pump guidance. The resulting core and cladding numerical apertures were 0.075 and 0.23 respectively. An aluminium coating was applied directly to the active fibre during draw using the freeze technique [4], ensuring good thermal contact and mechanical robustness.

The active fibre was drawn to a core diameter of 20  $\mu\text{m}$ , inner cladding diameter of 200  $\mu\text{m}$  and outer (fluorine doped glass) cladding diameter of 230  $\mu\text{m}$ . A cross-sectional view of this fibre is shown in Fig. 7. The relatively high core-to-clad area ratio of this fibre was chosen to ensure efficient pump absorption despite the low ytterbium concentration within the fibre core. At this cladding diameter the V-number of the active fibre core was 4.3 and thus multimode operation was expected.

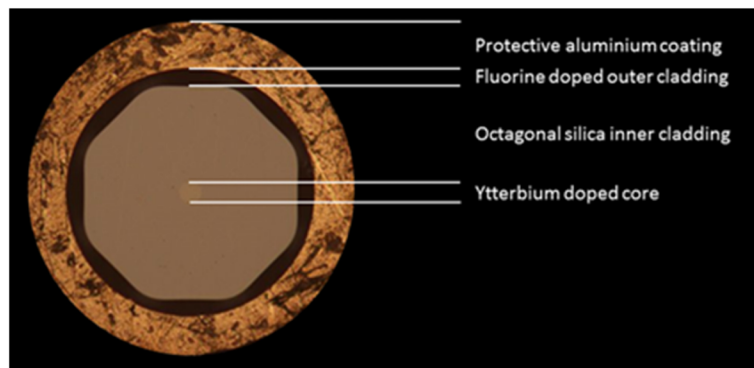


**Fig. 7.** Cross-sectional view of the metal coated active fibre with all-glass inner cladding and ytterbium doped core. Fibre dimensions were 20/200/230  $\mu\text{m}$  with numerical apertures of 0.075 and 0.23 for core, inner cladding and outer cladding respectively.

### 3.2. High temperature operation of an all-glass fibre laser

As part of the thermal analysis presented in Section 2, the active fibre core temperature was estimated as a function of both fibre design and thermal load. However, this analysis is incomplete without also studying any effects core temperature has on laser performance.

Moore [21] and Newel [22] have both presented detailed spectroscopic studies of ytterbium-doped silica at elevated temperatures with Moore presenting data on absorption and emission spectra as well as upper state lifetimes for temperatures up to 1000  $^{\circ}\text{C}$ , here it was found that a steep decline in upper state lifetime occurs at around 500  $^{\circ}\text{C}$ . Due to increasing short wavelength reabsorption, the gain peak of these fibres was red shifted toward longer wavelengths as well. By removing the polymer outer coating, Moore was able to investigate laser performance at elevated temperatures. However the use of an essentially unclad active fibre resulted in reduced slope efficiencies ( $\sim 20\%$ ) as well as a high degree of variability in pump absorption measurements. The all-glass cladding of the active fibre we have described above presents an ideal candidate for the continuation of this work, allowing more detailed laser performance and slope efficiency measurements. Here the all-glass cladding allows the effects of cladding loss and laser performance to be more easily distinguished. The high temperature behaviour of an all-glass clad ytterbium active fibre is investigated in this section by placing the active fibre in a temperature controlled oven and monitoring laser performance as a function of heatsink temperature. Laser threshold, slope efficiency and free running wavelength were all recorded as a function of furnace temperature over a temperature range of 25 – 400  $^{\circ}\text{C}$ .

For these high temperature experiments we opted to first remove the metal outer coating of the active fibre. This allowed us to separate out any effects the metal coating might have on laser performance more clearly highlighting spectroscopic effects.

An active fibre length of 11 m was used with approximately 10 m of this fibre first spooled to a diameter of 20 cm and then placed in the oven in thermal contact with the heating element. The remaining fibre lengths enabled in and out coupling of both the pump and signal light. A linear cavity was constructed containing a flat cleave at the laser output for output coupling ( $R \sim 4\%$ ) and an external cavity containing a broadband high reflector. A 60 W fibre coupled 975 nm diode (IPG) was used as the laser pump source and was directly coupled into the cladding of the active fibre using a pair of AR coated aspheric lenses ( $f = 25$  mm) with a coupling efficiency of 95%. At both ends of the laser cavity dichroic mirrors were used to separate pump and signal light and thermal power meters were used to record laser output and residual pump light.

Low power operation was maintained to minimise the effects of self-heating due to the quantum defect. Further details of this experimental arrangement and the furnace design can be found in [23].

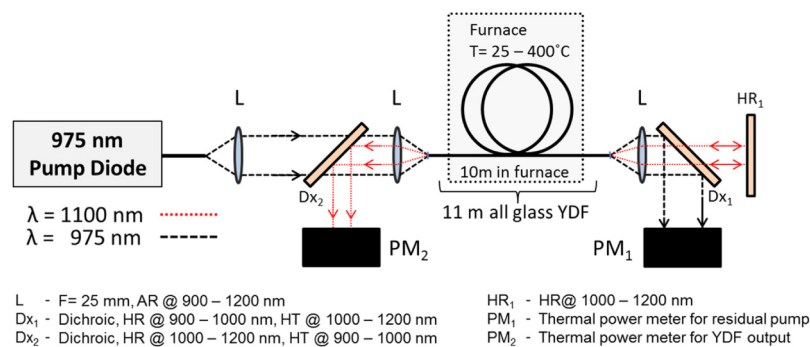


**Fig. 8.** Schematic of high temperature all-glass fibre laser slope efficiency measurements and diagnostics.

### 3.3. Metal clad ytterbium fibre laser

To allow investigation into any effects of metal coating has on laser performance a comparison was made between metal coated and all-glass fibre laser. Here the furnace was removed from the laser cavity but all other components were maintained identically to that described in Fig. 8. Laser slope efficiency and threshold was then recorded for an 11 m length of metal coated active fibre.

### 3.4. High power metal clad fibre laser

With an experimental layout similar to that used in the previous section the low power 60 W fibre coupled diode was replaced with a high brightness 750 W pump diode (DiLas). This diode source was fibre coupled to a 200  $\mu$ m diameter 0.22 NA passive fibre. To accommodate the higher power density of this diode larger aperture aspheric lenses were used with focal lengths of 40 mm. An additional water cooled aperture ( $\phi$  20 mm) was also placed after the first collimating lens to prevent excess NA light from reaching the active fibre and causing damage. As a precaution several bandpass filters centred at 975 nm (Edmund Optics, 50 nm FWHM) were also placed in the optical path as a means of pump protection. A diagram of this experimental layout can be found in Fig. 9. After lenses, aperturing and filtering  $\sim 650$  W was incident on the active fibre. Of this  $\sim 570$  W of pump light was estimated to be coupled into the active fibre (as measured using a 0.22 NA 200  $\mu$ m passive fibre). These values correspond to through transmission and coupling efficiencies of 86% and 88% respectively. In order to ensure complete pump absorption the metal coated active fibre length was increased to  $\sim 20$  m and was loosely coiled to a diameter of 20 cm. This coil was placed in thermal contact with the optical bench and forced airflow used for thermal management. Again a

simple end pumped cavity containing a 4% output coupling and a highly reflective external cavity feedback was chosen.

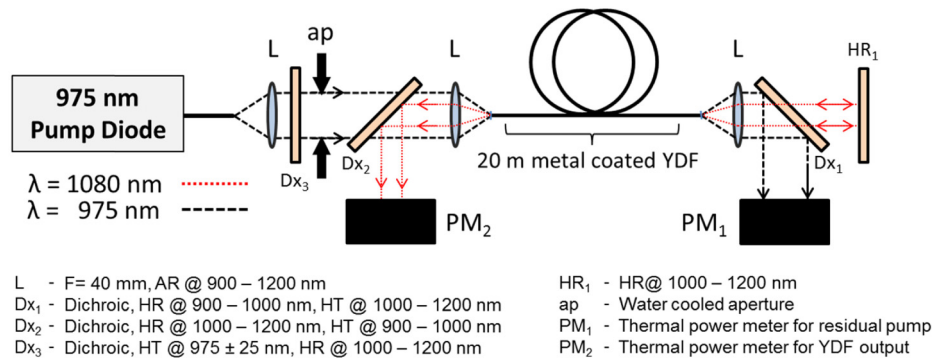


**Fig. 9.** Experimental layout for both high power conductively and passively cooled ytterbium fibre laser measurements.

### 3.5. Ultralight fibre laser demonstrator

One of the major advantages of the metal cladding approach is the improved thermal handling of the active fibre. As an investigation of this, a compact light weight laser gain module was constructed. This was designed to take advantage of both the increased temperature handling and thermal performance and of the metal coated fibre as well as the remarkable insensitivity to operating temperature that ytterbium fibre lasers can show [23].

In this section we investigate the performance of a passively (primarily radiatively) cooled ytterbium fibre laser. Using an optical configuration identical to that in the previous section the active fibre was now mounted into a planar arrangement in a light-weight high emissivity heatsink design that incorporated both high operating temperature and excellent thermal performance. The resulting laser gain module had a surface area of 650 cm<sup>2</sup> and weighed less than 100 g. To minimise the effects of conductive cooling, this gain module was suspended ~80 mm above the optical bench using four 6 mm diameter stainless steel posts and care was also taken to minimise any air flow about the heatsink. ~30 cm lengths of uncoiled fibre were used as a lead-in and lead-out for the free-space launching of pump light and to couple to the external feedback cavity. These sections were conductively cooled by being placed in thermal contact with the optical bench.

## 4. Results

### 4.1. High temperature all-glass fibre laser

At room temperature the active fibre produced a laser slope efficiency of 82% (with respect to absorbed pump power) and a maximum output power of 43.6 W. whilst maintaining maximum pump power, the active fibre heatsink was increased from room temperature up to a maximum temperature of 400°C. Over this range a linear reduction in laser output power was seen (~14 mW/°C) and at maximum heatsink temperature the laser output power was 38.5 W. This reduction in laser output power was a combination of reduced pump absorption and increased laser threshold and quantum defect. With this in mind the laser slope efficiency as a function of absorbed pump power was also recorded. Here we see only a slight decline in laser slope even at extreme operating temperatures. For a heatsink temperature of 400°C the laser slope efficiency was recorded to be 78% (i.e. only a 4% reduction in slope across a ~400°C temperature span).

The free running wavelength of this source (shown in Fig. 10(b.insert)) showed a trend towards longer wavelengths as a function of heatsink temperature with the central wavelength shifting from 1087 nm at room temperature to 1113 nm at 400°C. This behaviour is discussed

in more detail in [5]. With the above wavelength shift corresponding to a  $\sim 2\%$  increase in quantum defect, this shift to longer wavelengths partly explains the reduced laser slope efficiency seen at higher temperatures.

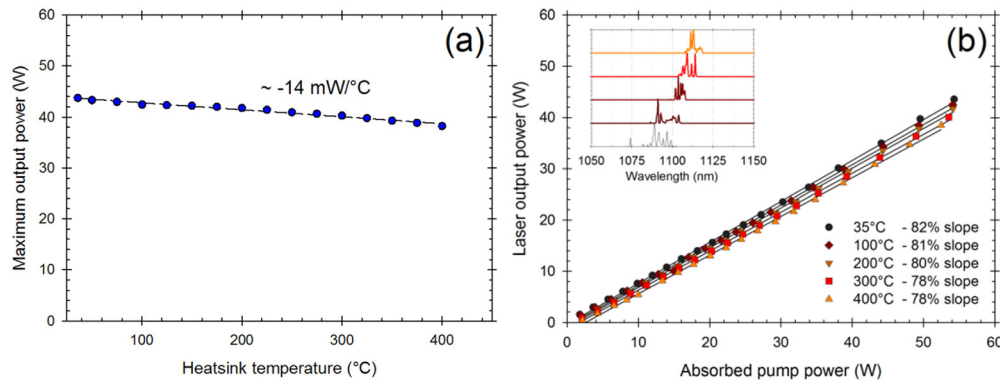


**Fig. 10.** a) Laser output power for a fixed launched pump power of 57.4 W and increasing heat-sink temperature. b) Laser slope efficiency as a function of heat-sink temperature from 35°C to 400°C. (Insert) free running laser wavelength as a function of heatsink temperature.

#### 4.2. Impact of metal coating on laser performance

A 10 m length of metal coated active fibre was loosely coiled onto the optical bench and the laser slope efficiency was recorded with results shown in Fig. 11. The corresponding slope efficiency with respect to the absorbed pump power was 81% (in comparison to 82% as measured for the all-glass case) confirming that the metal cladding had only minimal impact to laser slope efficiency.

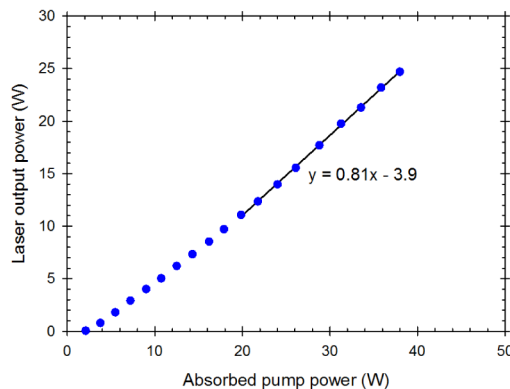


**Fig. 11.** Laser slope efficiency as a function of absorbed pump power for the metal coated active fibre.

#### 4.3. Metal clad fibre laser power scaling

At a maximum coupled pump power of 570 W this source provided up to 415 W of output power at a central wavelength of 1080 nm. Laser slope efficiency and beam profile are shown in Fig. 12(a) and Fig. 12(b) respectively. A laser slope efficiency of  $\sim 74\%$  was recorded for this high power result. This reduction in laser slope efficiency in comparison to the lower power result can be seen as a combination of excess fibre device length (chosen to ensure complete pump absorption) and uncertainty in pump coupling efficiency. With further optimisation or by moving to an all-fibre design a laser slope efficiency closer to 80% is expected. At maximum pump power the laser output was a doughnut shaped beam with partially filled central region and suspected to be an incoherent combination of  $LP_{01}$  and  $LP_{11}$



mode groups [24]. Linear fitting to this profile suggests an  $M^2$  of between  $M^2 \sim 1.0 - 2.5$ . It is interesting to note that such doughnut shaped beam profiles, which are a topic of continuing interest to the industrial laser community, may be beneficial for machining applications [25] due to favourable thermal and processing properties. In this experiment the purity of this doughnut shaped output was found to be dependent on the flatness of the optical fibre cleave angle. As has been shown elsewhere it may be possible to further refine this laser output profile using an appropriate external cavity design [26].

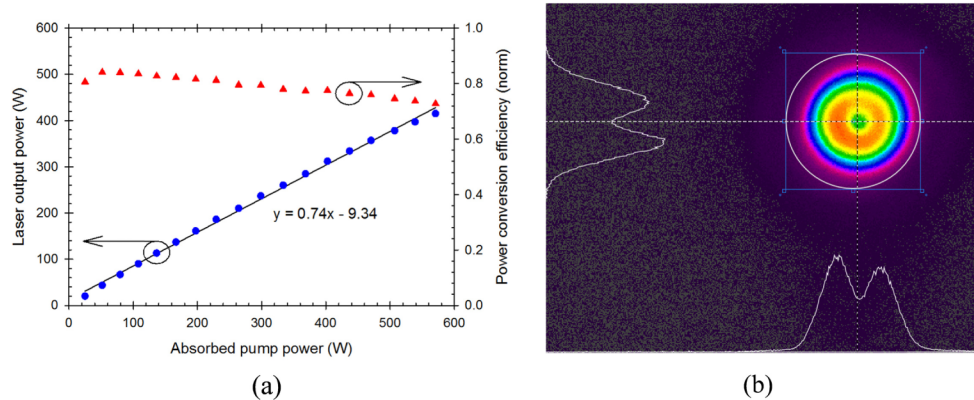


**Fig. 12.** a) Laser slope efficiency as a function of absorbed pump power (left axis) and laser power conversion efficiency (right axis). b) Laser output beam profile at maximum pump power.

#### 4.4. Passively cooled ultralight fibre laser demonstrator

The laser output power and thermal performance of the light-weight laser gain module was recorded as a function of pump power. At a maximum launched pump power of 570 W the passively cooled laser gain module was able to produce 405 W of signal light showing almost no impact to laser performance in comparison to the previous air cooled result. A thermal profile of this module is shown in Fig. 13. Here we can see a maximum heat-sink temperature of  $\sim 140^\circ\text{C}$  under a total thermal load of  $\sim 150$  W. This gain module was operated over a period of 20 mins without signs of degradation.

Ultimately thermal damage occurred on a lead in section to the fibre gain module that was suspended in free space, here the low emissivity of the polished metal coating acted as thermal insulator and thermal runaway occurred in the absence of airflow. Before damage, this section reached an estimated temperature of  $800 - 1000^\circ\text{C}$  based on the cherry red emission of the aluminium coating. This coincided with the onset of a slow decay in laser output power and was maintained for several minutes before the lead-in fibre failed.

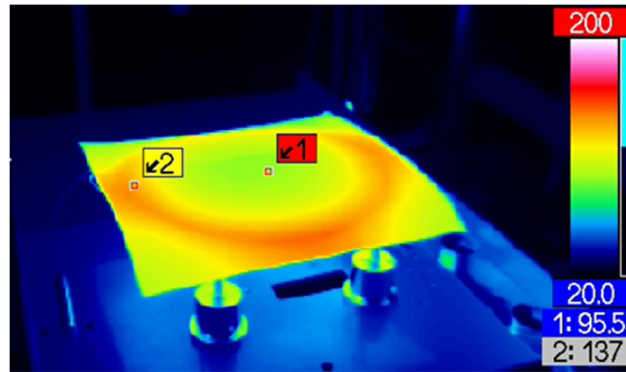


**Fig. 13.** Thermal profile of ultralight fibre gain module operating at a output power of 405 W and maximum operating temperature of 137 °C

## 5. Discussion

By removing fluoropolymers from active and passive fibre design it is possible to manufacture more robust laser systems whilst also removing excess weight associated with cooling requirements. Although in this initial demonstration we have opted for a free-space design we are in the process of building up the componentry needed for metal coated all-fibre laser systems. This includes investigations into the use of metal coated passive fibre for laser diode beam delivery, metal coated tapered fibre bundles and metal coated fibre Bragg grating packages. We are also investigating the ability to ‘recoat’ any stripped fibre sections using low melting point metals resulting in robust splice points with very high thermal conductivity. By building up this infrastructure and componentry, issues such thermal management of excess pump light at splices and within tapered fibre bundles is greatly reduced leading to simplified and very light weight systems. Within the diode laser community, several research groups are also actively pursuing high power density [27], light weight [28] and high operating temperature [29] diode packages. All which serve to complement the work presented here and once combined have the potential to enable significantly more compact and efficient fibre laser systems.

Whilst ytterbium fibre lasers operating in the more four-level regime ( $\lambda \approx 1070$  nm) show only a weak dependence on operating temperature for slope efficiency, other dopants with more complex spectroscopy tend to show stronger thermal dependence. For example, Thulium has shown a far greater sensitivity to operating temperature and heat removal, with the authors from [30] noting a 1.6 times increase in laser slope efficiency when improved cooling was used. Finally soft glass laser systems such as Er:ZBLAN with their low thermal conductivity, high thermal load and low melting point are an ideal candidate for metal coated fibre designs. In addition to the beneficial thermal properties of metal coated active fibres the ability to hermetically seal the active fibre from surface oxidation and hydrogen / water ingress is also an interesting prospect.

## 6. Conclusion

We have presented modelling and the first detailed demonstration of a high power metal clad fibre laser. By removing the high thermal sensitivity fluoropolymer cladding we can significantly reduce the maximum core operating temperature. In addition to this we are also able to operate the fibre laser over a much wider range of temperatures and under much higher thermal loads. We initially investigate the thermal sensitivity of an all-glass ytterbium fibre laser through actively heating the gain fibre. With a laser slope efficiency of 82% at room temperature and 78% at a heatsink temperature 400°C we confirmed that only a minimal thermal dependence is seen and corresponds to only a 1% reduction in slope

efficiency per 100°C of operating temperature. Metal coating of an active fibre significantly improves fibre strength and handling and through comparison of laser performance between the all-glass and metal coated designs we noted negligible impact to laser performance.

As a demonstration of the capabilities of this metal coated fibre, we ran for the first time to the best of our knowledge a high power ytterbium fibre laser operating in a completely passively cooled configuration. Using primarily radiative cooling as a heat removal method, this configuration produced a pump power limited 405 W of laser output power and laser slope efficiency of 74%. This compact ultra-light weight laser package weighed in at less than 100 g. Modelling conducted on this package suggests with further optimised active fibre, 1kW level output powers are possible. Without significant changes to laser design this would correspond to power to weight ratios of  $> 100$  g/kW of the active fibre laser head. In addition to the weight savings achieved the high operating temperature range of metal coated active fibres opens up new opportunities for wavelength flexibility and non-linear suppression. Demonstrations of a ~40% increase in wavelength tunable operating bandwidth and estimated SBS non-linear suppression factors of up to 7-10 dB are possible.

Metal coated active fibres open up a new operating area for high power fibre laser systems, with a new design space for non-linear suppression, power scaling and ultra-light fibre laser designs now accessible.